An improved algorithm for computing local fractal dimension using the triangular prism method

Wenxue Ju [a,1], Nina S.-N. Lam [b,*]

[a] *Department of Geography and Anthropology, Louisiana State University, Baton Rouge, LA 70803, USA*
[b] *Department of Environmental Sciences, Louisiana State University, Baton Rouge, LA 70803, USA*

ARTICLE INFO

ABSTRACT

Despite the many applications of fractals in geosciences, the problem of inconsistent results derived from different fractal calculation algorithms remains. Previous research found that the modified triangular prism method was the most accurate for calculating the fractal dimension of complex surfaces such as remote sensing images. However, when extending the application of the technique into local measurements, new problems arise. Hence, adjustment to the existing technique is needed. This paper introduces a new algorithm for calculating the fractal dimension within a local window based on the triangular prism method. Instead of using arbitrary geometric steps, the new algorithm computes the number of steps needed for fractal calculation according to the window size. The new algorithm, called the divisor-step method, was tested using 4000 simulated surfaces and found to be more robust and accurate than the conventional geometric-step method. The new divisor-step method is recommended especially for local measurements.

© 2009 Elsevier Ltd. All rights reserved.

1. Introduction

As a promising spatial metric, the fractal dimension (Mandelbrot, 1967) has been frequently applied in many geoscience applications, including remote-sensing image-complexity characterization (De Cola, 1989; Lam, 2004; Liu and Cameron, 2001; Qiu et al., 1999; Quattrochi et al., 2001; Turner and Ruscher, 1988), land use/land cover classification, and change detection (Chust et al., 2004; Emerson et al., 2005; Myint et al., 2004; Myint and Lam, 2005; Read and Lam, 2002). Despite the many applications, the problem of inconsistent results derived from different fractal calculation algorithms remains. Algorithms such as the isarithm, variogram, probability,

box-counting, and triangular prism methods have been proposed and tested (Goodchild, 1980; Jaggi et al., 1993; Lam and De Cola, 1993; Sun et al., 2006; Tate, 1998; Voss, 1988). For complex surfaces such as remote sensing images, it was found that the modified triangular prism method was the most reliable estimator when compared with the isarithm and variogram methods (Lam et al., 2002; Zhou and Lam, 2005). This paper focuses on improving the triangular prism method, especially on extending its applications for local measurements.

Originally proposed by Clarke (1986), the triangular prism method utilizes imaginary three-dimensional prisms constructed from the image, and then compares the total prism surface area with the step size used to derive the prisms in a double-logarithmic regression. The slope of the regression is then used to estimate the fractal dimension. Specifically, a triangular prism is constructed by connecting four adjacent pixels and its center (Fig. 1). The height of each corner pixel is the pixel intensity value and the height of the center takes the average of the four

---

* Corresponding author. Tel.: +1 225 578 3030; fax: +1 225 578 4286.
 E-mail addresses: wju1@lsu.edu (W. Ju), nlam@lsu.edu (N.S.-N. Lam).
 [1] Current address: ESRI, Inc., 380 New York Street, Redlands, CA 92373, USA.
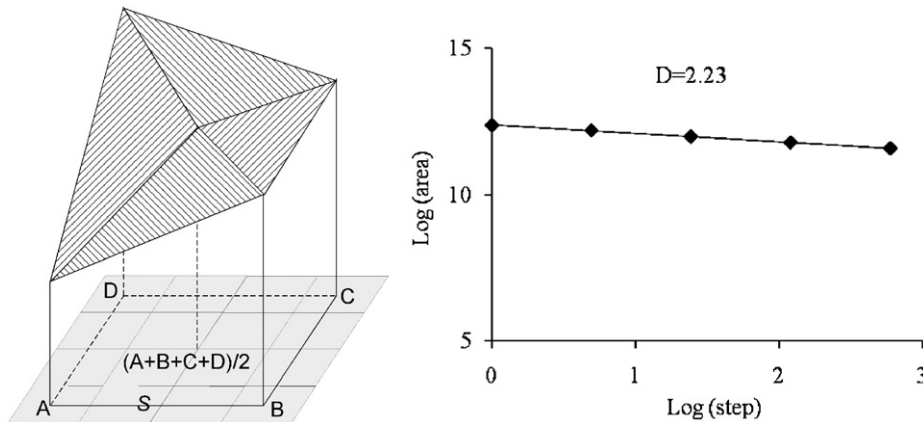
Fig. 1. A triangular prism and a regression plot.

corner pixels. The step size is the number of pixels on a side. Given a step size, triangular prisms are constructed across the image and the total surface area of all triangular prisms calculated. The procedure is repeated for each step size. A double-log regression between the total prism surface area (A) and the area of step size (S^2) is estimated to derive the slope B, where fractal dimension $D = 2 - B$. Clarke's original algorithm was later modified so that the length of step size, not step-size squared, is used in the regression, because the use of step-size squared led to underestimation of the fractal dimension (Jaggi et al., 1993). The modified triangular prism method was subsequently proven to be mathematically correct, as well as experimentally reliable (Lam et al., 2002; Zhao, 2001). It was then suggested that the modified triangular prism method should be used. Hence,

$$\mathrm{Log}\,A = a + (2 - D)\mathrm{Log}\,S \qquad (1)$$

where A is the total surface area of the prism "facets", S is the step size, a is the intercept, and D is the fractal dimension. In the remainder of the paper, whenever the term "triangular prism method" is used, it implies the modified version. It is noted that some other variants were also developed by using alternative pixels other than corner pixels of the square (Sun, 2006).

In general, the triangular prism method is very robust in its estimation of the fractal dimension. The only source of estimation variation is the choice of the number of steps and the corresponding step sizes. How to determine these two related parameters so that the results are reliable is the focus of this study. In essence, this is an issue of sampling strategy, which is common to many fractal estimation algorithms and will affect the estimation accuracy. This paper introduces a new sampling strategy, called the divisor-step method, which is designed to overcome the weakness of the geometric-step method that has been commonly employed in the triangular prism method.

2. Sampling issues

The original algorithm by Clarke (1986) uses a series of geometric steps with an increase in power of two until it

reaches the maximum limit imposed by the algorithm. For example, for a 33×33 image, steps 1, 2, 4, 8, and 16 can be used. The maximum step size is usually bounded by a value equivalent to the image size minus one and divided by half ($(W-1)/2$), which is 16 in this case. Otherwise, it will result in only one triangular prism for the largest step ($S = 32$ for the example), which could lead to unstable log–log area-step regression. The use of geometric steps is to ensure that points are distributed uniformly on the log–log regression curve so that an unbiased regression can be obtained. However, if the size of an image (or local window within an image) is not of $2^n + 1$ pixels (for convenience, it is called "geometric-square" image thereafter), a portion of the image will not be included in the calculation. This is considered undesirable from a theoretical point of view, as variation in some parts of the image is not measured. When the algorithm applied locally to a small non-geometric-square local window, the omitted portion could be significantly large that could lead to unreliable estimation of local fractal dimension. For example, if the local window size is 29×29, using geometric steps of 1, 2, 4, and 8, only 17×17 (i.e., $2^n + 1$) pixels will be used, whereas the remaining 2/3 pixels within the window will not be included in the estimation.

Another sampling method is to employ arithmetic steps, such as 1, 2, 3, 4, and so on. The arithmetic-step method has an advantage that it can yield sufficient number of area-step points for the log–log regression even for a very small study area. However, since it is not a geometric progression, a counter argument for this method is that these arithmetic points might bias the log–log regression estimate as a result of including more samples at the lower end of the regression. The proposed divisor-step method is designed such that full coverage of the sampling area is ensured at each step.

3. Comparison using effective coverage ratio

3.1. The geometric-step method (fixed coverage)

The geometric-step method, as originally presented by Clarke (1986), requires the calculation to be based on a
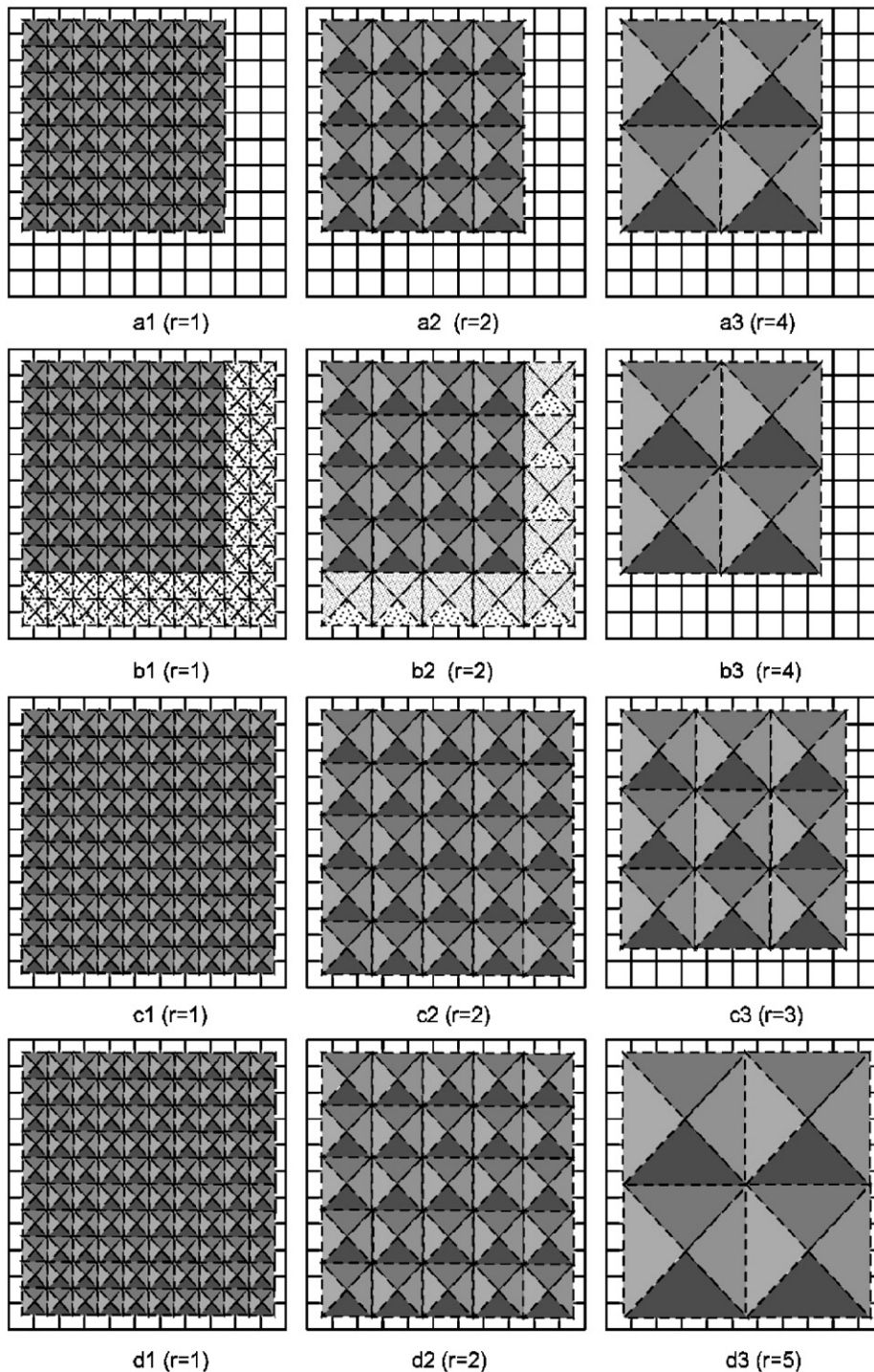
Fig. 2. A top-view demonstration of coverage (shaded prisms) by different sampling methods with an 11×11 window. (a1–a3): geometric-step method (fixed coverage); (b1–b3): geometric-step method (varying coverage); (c1–c3): arithmetic-step method; (d1–d3): divisor-step method.

geometric-square subset of the study area. It has a fixed coverage for all the geometric steps. Fig. 2a shows the geometric steps of 1, 2, and 4 for an 11×11 local window. For ease of visual comparison with other methods, the upper-left subset is used instead of center cut. It is

apparent from Fig. 2a that some pixels are "wasted" and will not be included in the calculation. As already mentioned above, this will cause two problems. First, the calculated fractal dimension is not a true measurement of the entire window, and second, local windows

with different sizes may have the same measurements as they may be confined by the same sampling sizes for calculation.

3.2. The geometric-step method (varying coverage)

To extend the ability of using geometric steps in the calculation of non-geometric-square windows, some algorithms will let the triangular prisms grow within the study area and cover as many pixels as possible. The coverage of triangular prisms at each step may vary, as illustrated in Fig. 2b. This method was implemented in the Image Characterization And Measurement System (ICAMS) software (Lam et al., 1998; Quattrochi et al., 1997). Although the coverage in this method is larger than that of the original algorithm, it is clear that complete coverage of the entire study area at all steps is not guaranteed.

3.3. The arithmetic-step method

The arithmetic-step method has been used in previous research to obtain sufficient number of regression points when using a small window (e.g., Emerson et al., 2005). The number of pixels utilized in the arithmetic-step method is generally more than that of the geometric-step methods. Fig. 2c presents the first three steps (1, 2, and 3) using the arithmetic-step method for the same 11×11 window. Similar to the geometric-step methods, however, 100% coverage of the entire window at all steps is not guaranteed.

3.4. The proposed divisor-step method

This new sampling method is quite intuitive. To cover the entire $W \times W$ window (W is an odd number) by triangular prisms at any given step, the step size should be a divisor of $(W-1)$. Using a set of divisor steps of $(W-1)$ will guarantee 100% coverage of the entire window at all steps. For this example, the three divisible steps are 1, 2,

and 5 (Fig. 2d). By taking advantage of the 100% window coverage at all steps, the derived fractal dimension value is expected to measure more accurately the surface variation within the study area. This is especially critical to local fractal estimation, as excluding some pixels for calculation in a small window area is more likely to lead to unreliable results.

3.5. Effective coverage ratio and coverage fluctuation

To quantify the effects of different algorithms on pixel utilization, the ratio between the average number of utilized pixels at each step and the total number of pixels contained in the local window can be used. In this study, we define this ratio as effective coverage ratio (ECR)

$$ECR = \left\{ \sum_{i \in \{s\}} \{floor[(W-1)/i] \times i + 1\}^2 / n \right\} \Big/ \{W \times W\} \quad (2)$$

where $\{s\}$ is the collection of step length, $\{floor[(W-1)/i] \times i+1\}^2$ is the coverage (in pixels) at a given step i, n is the size of the collection $\{s\}$, W is the size of the local window. Higher ECR means less-wasted pixels. For the geometric (fixed coverage) method, as the calculation is based on a square subset, the ECR is calculated as the following:

$$ECR = \{[floor(\log_2 W) + 1]/W\}^2 \quad (3)$$

Along with ECR, the standard deviation of coverage (SDC) for all steps for each method can be calculated. Table 1 lists the ECR and SDC of different methods at different window sizes. The divisor-step method has 100% coverage, whereas the geometric-step method (fixed coverage) has the largest waste of pixels (i.e., lowest ECR); hence, the method is not considered desirable and will not be further tested in the following with simulated surfaces. The arithmetic-step method and the geometric-step (varying coverage) generally have larger ECRs than the geometric-step method (fixed coverage). Neither the geometric-step (varying coverage) nor the arithmetic-step

Table 1
Effective coverage ratios (ECR) and standard deviation of coverage (SDC) of different sampling methods (%).

Window	Geometric (fixed)		Geometric (varying)		Arithmetic		Divisor	
	ECR	SDC	ECR	SDC	ECR	SDC	ECR	SDC
9×9	100	0.00	100	0.00	90.12	1.23	100	0.00
13×13	47.93	0.00	100	0.00	95.27	0.48	100	0.00
17×17	100	0.00	100	0.00	89.19	0.49	100	0.00
21×21	65.53	0.00	91.38	0.17	86.21	0.47	100	0.00
25×25	46.24	0.00	100	0.00	88.41	0.34	100	0.00
29×29	34.36	0.00	93.58	0.13	85.13	0.30	100	0.00
33×33	100	0.00	100	0.00	83.79	0.28	100	0.00
37×37	79.55	0.00	91.82	0.11	87.63	0.23	100	0.00
41×41	64.78	0.00	92.96	0.16	84.87	0.22	100	0.00
45×45	53.78	0.00	87.36	0.20	82.15	0.20	100	0.00
49×49	45.36	0.00	100	0.00	84.76	0.18	100	0.00
53×53	38.77	0.00	94.19	0.08	82.87	0.16	100	0.00
57×57	33.52	0.00	94.78	0.12	83.84	0.16	100	0.00
61×61	29.27	0.00	90.37	0.15	84.92	0.14	100	0.00
65×65	100	0.00	100	0.00	82.72	0.14	100	0.00
69×69	88.74	0.00	94.37	0.06	81.49	0.13	100	0.00

method can guarantee a full coverage for all steps. The ECR and coverage fluctuation (SDC) are expected to affect the accuracy and robustness of subsequent fractal surface dimension estimation.

4. Comparison using simulated images

4.1. Shear displacement simulation

Since simulated self-similar fractal surfaces have frequently been used for benchmark testing, we will also utilize these simulated surfaces to test the performance of the different sampling methods (Lam et al., 2002; Zhou and Lam, 2005). The shear displacement method is one of the popular algorithms used to generate fractional Brownian motion (fBm) surfaces (Mandelbrot, 1975, 1983; Goodchild, 1980; Lam and De Cola, 1993). The

algorithm works as follows: an image is initialized with zero values everywhere. The image is then randomly cut into halves and each part is randomly shifted vertically. This shear-and-displacement process is repeated a number of times until there are several cliffs between adjacent pixels. A Poisson process controls the intersection points of the break lines, while the angles of intersections are uniformly distributed. A persistence factor H controls the magnitude of vertical shift and H satisfies

$$E(Z_i - Z_{i+d})^2 = |d|^{2H} \qquad (4)$$

where Z_i is the pixel value and d is the pixel distance. The expected variance between two pixels is a function of their distance powered by $2H$. Fractal dimension is $3\text{-}H$.

The shear displacement algorithm has been implemented in ICAMS (Lam et al., 1998; Quattrochi et al., 1997) with a batch mode available. Fig. 3 shows a set of 45×45
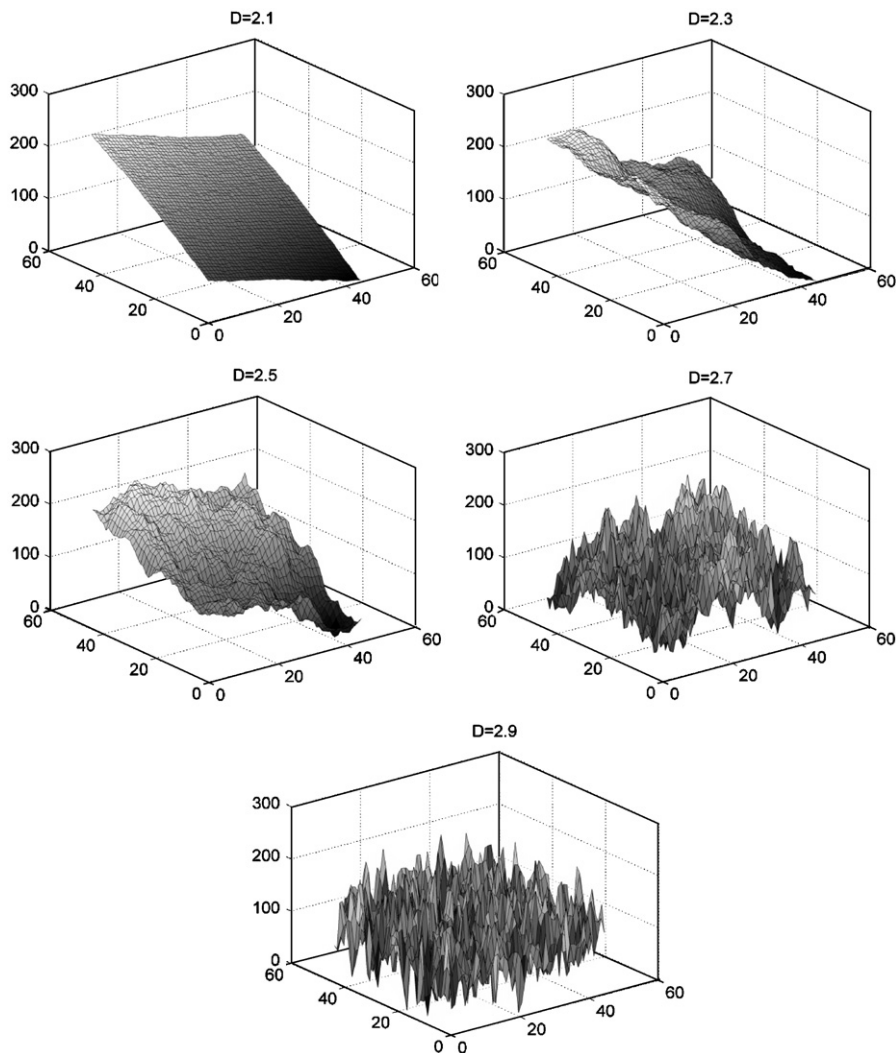
Fig. 3. Fractional Brownian surfaces (45×45) generated using shear displacement algorithm (3000 cuts).

fractal surfaces with varying levels of complexity generated using ICAMS.

4.2. Comparison among different sampling methods

To compare the accuracy and robustness of different sampling methods, a set of small simulated surfaces with 16 sizes ranging from 9×9 to 69×69 were generated. These window sizes were selected, because this series cover most windows used in the previous image classification or segmentation research that uses local fractal measurements (De Jong and Burrough, 1995; Emerson et al., 2005; Myint and Lam, 2005). For each window size, 50 surfaces were generated for each of the five theoretical dimensions (2.1, 2.3, 2.5, 2.7, and 2.9) using the same number of cuts (3000). The 50 surfaces were generated with the same control parameters (theoretical dimension, image size, and number of cuts), but each time a different sequence of random numbers was used, hence the surfaces are different. The surfaces were generated by ICAMS based on the algorithm described in Lam and De Cola (1993). This resulted in a total of 4000 surfaces used for this experiment. All simulated surfaces were stretched to 0–255 to provide the same basis for comparison. For the geometric-step (varying coverage) method, the maximum number of steps and step sizes were calculated according to $(W-1)/2$, and in this experiment, the number of steps ranged from 4 to 6 (except when $W = 9$), depending on the window size. For the arithmetic-step method, the number of steps was $(W-1)/2$. The number of steps of the divisor-step method depended on the available divisors of $(W-1)$, and it ranged from 4 to 11 (except when $W = 9$) in this experiment. ICAMS was used to generate the simulated surfaces. ICAMS already has two built-in modules for the geometric-step (varying coverage) and arithmetic-step methods. The divisor-step method was programmed in Matlab and was not yet available in ICAMS. Sample code can be requested from the authors.

For each window size, the average estimated fractal dimension was calculated and the root-mean-square errors between the estimated and the theoretical D were computed. The grand average values by fractal dimension for all window sizes are presented in Table 2. Based on the average estimated D measure, the arithmetic-step method yielded an estimated fractal dimension much closer to the

theoretical D for surfaces with low complexity (when $D < 2.5$), whereas the divisor-step method yielded more accurate estimates for surfaces with high complexity (when $D > 2.5$). This pattern can also be reflected by the average RMSE measure, where the divisor method resulted in lower RMSE for surfaces with high complexity, and the arithmetic-step method yielded lower RMSE for surfaces with low complexity. The geometric-step method (varying coverage) ranks in the middle, with a grand average RMSE equals to 0.132, compared with 0.123 and 0.136 of the divisor-step and arithmetic-step methods, respectively.

A closer look of the results across window sizes provides further insights. Fig. 4 plots the mean estimated fractal dimension from different algorithms at different windows. It can be observed that the geometric-step method (varying coverage) had the most unstable estimation across different window sizes and yielded the largest deviations from the theoretical values at most window sizes. The three peak points of the geometric-step method (varying coverage) corresponded to the three worst ECR and SDC in Table 1 (at windows 21×21, 45×45, and 61×61). This implies that the geometric-step (varying coverage) method tends to overestimate the fractal surface dimension ($D = 2.7, 2.9$) when there is uneven or partial coverage among the steps. When the coverage is about the same as in other methods (arithmetic and divisor), the geometric-step (varying coverage) method yields similar fractal dimension values, as expected.

The arithmetic-step method consistently yields higher estimated fractal dimension than the divisor-step method across all window sizes. The plot (Fig. 4) further confirms that the arithmetic-step method is a more accurate estimator for low-complexity surfaces across all window sizes, whereas the divisor-method is more accurate for high-complexity surfaces. The estimates from the geometric-step (varying coverage) method fluctuate a lot across the windows, making this method far less desirable for fractal surface estimation.

The RMSE plots across windows (Fig. 5) also show similar patterns. For surfaces with high complexity ($D = 2.7, 2.9$), the arithmetic-step method is clearly the worst due to high RMSEs and overestimation. The geometric-step (varying coverage) method also yielded high RMSEs, especially for windows with low ECRs and high SDCs (e.g., at 21, 45, and 61). The divisor-step method

Table 2
Estimated fractal dimension and RMSE averaged for all 16 window sizes (from 17×17 to 69×69).

D	Geometric (varying)		Arithmetic		Divisor	
	Average D	Average RMSE	Average D	Average RMSE	Average D	Average RMSE
2.1	2.12	0.109	2.15	0.101	2.04	0.095
2.3	2.18	0.153	2.24	0.109	2.11	0.201
2.5	2.45	0.129	2.53	0.111	2.39	0.141
2.7	2.79	0.143	2.87	0.195	2.74	0.101
2.9	2.97	0.127	3.06	0.166	2.91	0.077
Grand average		0.132		0.136		0.123
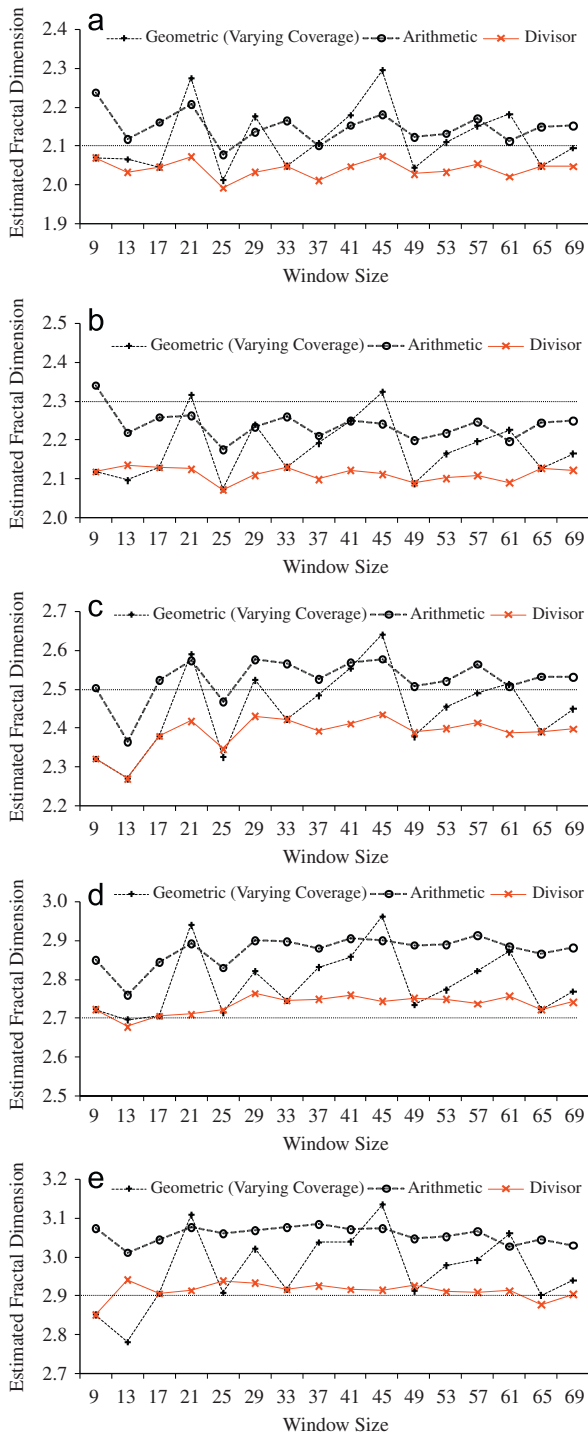
Fig. 4. Mean estimated fractal dimensions derived from different methods, theoretical dimension shown in dashed straight line: (a) $D = 2.1$; (b) $D = 2.3$; (c) $D = 2.5$; (d) $D = 2.7$; and (e) $D = 2.9$.

Fig. 5. RMSE of different methods: (a) $D = 2.1$; (b) $D = 2.3$; (c) $D = 2.5$; (d) $D = 2.7$; and (e) $D = 2.9$.

is generally the best for most windows. For surfaces with medium–low complexity ($D = 2.3$, 2.5), the arithmetic-step method generally achieves the best RMSE for most windows. For surfaces with $D = 2.1$, the arithmetic-step method is close to the divisor-step method.

Based on this experiment, we can conclude that the geometric-step method (varying coverage) is most unstable across different local windows and is less accurate than the others for most theoretical dimensions, thus the method should be avoided in the future.

The arithmetic-step method consistently yields a higher estimate than the other methods and is generally a better estimator for surfaces with medium–low complexity ($D = 2.3$, 2.5), but it seriously overestimates the fractal dimension of surfaces with high complexity ($D = 2.7$, 2.9). For $D = 2.9$, the estimation consistently exceeds the theoretical maximum of 3.0. The divisor-step method is generally the best for surfaces with high complexity ($D = 2.7$, 2.9) and very low complexity ($D = 2.1$), but it underestimates for surfaces of medium and low complexity (for $D = 2.3$ and 2.5 with few exceptions).

5. Comparison with real-world data

To illustrate the effects of different algorithms in the real-world situation, a test was made using an IKONOS image (Fig. 6a). The subset (252×252 pixels) is the near-infrared band of a typical urban residential neighborhood extracted from an IKONOS image of New Orleans,

Louisiana. The bit depth of the IKONOS image is 11-bit, and the spatial resolution of the near-infrared band is 4 m. The residential neighborhood exhibits a fractal appearance.

To visualize the difference among different sampling methods in generating fractal layers, a 21×21 pixels moving-window was applied to the subset to compute local fractal dimensions using different sampling methods. The 21×21 window size was picked because it was one of the three peak points at which the performance of the geometric-step method (varying coverage) was the worst (Fig. 4). The use of this window size is expected to better illustrate the problem of the geometric-step method (varying coverage) visually. The results were scaled to 0–255 for display (Fig. 6). The overwhelming brighter appearance of the geometric-step (varying coverage) and the arithmetic-step methods over the divisor-step method indicate higher estimated values, a finding similar to that of the simulated surface experiment. The standard deviations of the estimated local
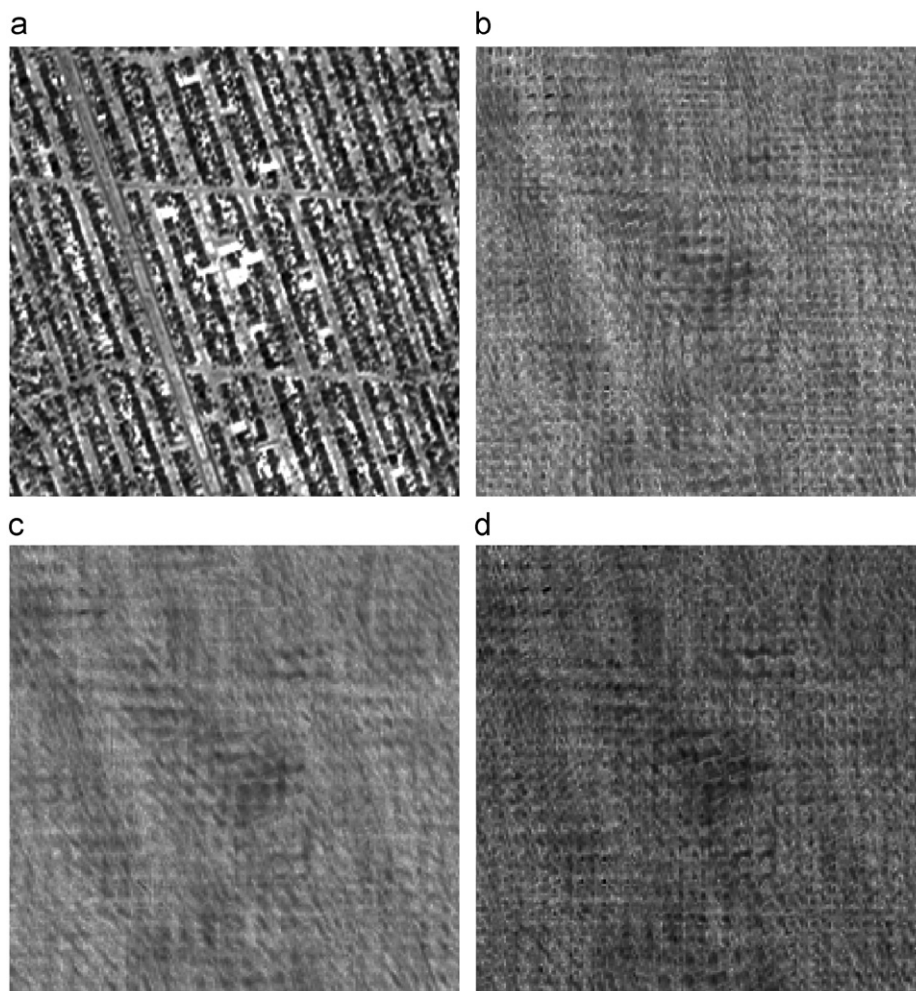
Fig. 6. (a) An urban residential neighborhood (252×252 pixels) displayed using near-infrared band of an IKONOS image from New Orleans, Louisiana, and fractal layers derived from using 21×21 moving-windows with different sampling methods; (b) geometric-step (varying coverage); (c) arithmetic-step; and (d) divisor-step. For (b) to (d), brighter pixels denote higher local fractal dimensions. (IKONOS satellite imagery courtesy of Geoeye.)

Table 3
Average local fractal dimension of a residential neighborhood in New Orleans, LA.

Window	Geometric (varying coverage)	Arithmetic	Divisor
9 × 9	2.52	2.67	2.52
13 × 13	2.51	2.68	2.59
17 × 17	2.65	2.79	2.65
21 × 21	2.84	2.85	2.68
25 × 25	2.64	2.87	2.72
29 × 29	2.77	2.90	2.72
33 × 33	2.74	2.93	2.74
37 × 37	2.84	2.93	2.77
41 × 41	2.87	2.95	2.76
45 × 45	2.95	2.96	2.78
49 × 49	2.73	2.97	2.80
53 × 53	2.80	2.98	2.80
57 × 57	2.82	3.00	2.79
61 × 61	2.88	3.00	2.83
65 × 65	2.81	3.00	2.81
69 × 69	2.85	3.01	2.82
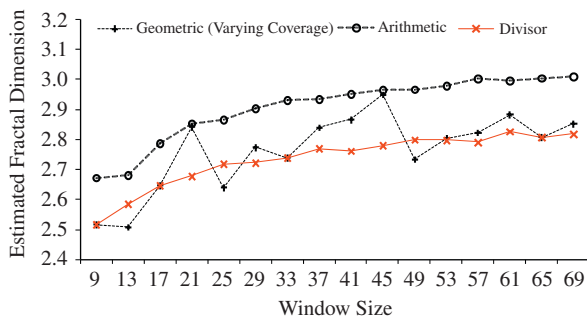
Fig. 7. Average fractal dimension of an urban residential neighborhood measured from near-infrared band of an IKONOS image in New Orleans, Louisiana.

fractal dimensions were computed. For stretched images (Fig. 6), the geometric-step method had the highest value (9.03), compared with 8.34 and 8.71 for the arithmetic-step and the divisor-step methods, respectively. Since the original image is quite self-similar (Fig. 6a), it is expected, local textures as reflected from the local fractal dimensions should be similar or stable across the image, hence the geometric-step method (varying coverage) can be interpreted as less reliable at this window size. It is noted that other factors such as variation of land cover, in addition to window size, may also contribute to higher standard deviation.

To further compare the estimated local fractal dimensions, 16 local windows ranging from 9 × 9 to 69 × 69 (in pixels) were used to derive fractal layers from the residential subset. As different windows leave different edge portions uncalculated, the central 150 × 150 pixels were extracted from the resultant layers to provide the same basis for comparison. The average local fractal dimensions of each window size are listed in Table 3 and plotted in Fig. 7.

Since this is a real-world data set that does not have a known D value to serve as a benchmark, comparison of different methods cannot be based on the accuracy of

estimated fractal dimensions. However, Table 3 and Fig. 7 clearly show that the geometric-step (varying coverage) method resulted in higher fluctuations in the average local fractal dimensions across windows. This result is similar to the results found in the simulated surface experiment and can be attributed to the problem of different coverage sizes at different sampling steps. The fluctuation across windows, which may be attributed largely to the sampling method, complicates the interpretation of window size effects. It added an algorithm effect in addition to the window size effect (Sun et al., 2006). Both the arithmetic-step and divisor-step methods yielded fractal dimension estimates that increased gradually with increasing window size while approaching a stable stage at larger windows. Similar to the simulated surface experiment, the arithmetic-step method seems to overestimate the fractal dimension for larger windows, with values exceeding 3.0, when window size is 57 × 57 and greater. Hence, from this comparison, it can be suggested that the divisor method is more preferable for real-world urban remote sensing application.

The above discussion has been focused on square images. In many geoscience applications, rectangular images are often used instead. Some other fractal dimension estimators can compute fractal dimensions of rectangular images easily, such as the isarithm and variogram estimators (Goodchild, 1980; Jaggi et al., 1993; Lam and De Cola, 1993). For the triangular prism method, the effects of sampling strategy on the resultant fractal estimates are expected to be greater for a rectangular image than for a square image. Eq. (2) can also be applied to evaluate the effective coverage ratio of rectangular image. Consider a 151 × 201 image, by applying Eq. (2), the ECRs for different methods can be computed as: 54.8% for the geometric-step method (fixed coverage), 82.0% for the geometric-step method (varying coverage), 93.0% for the arithmetic-step method, and 100% for the divisor-step method (using common divisors of both sides). For irregular shapes, the triangular prism method would not be an effective method for computing the fractal dimension. Alternative methods such as the isarithm method should be considered.

6. Conclusions

Fractal dimension as an index has been widely used in geosciences, even though inconsistent results from different fractal estimators remain. Such inconsistencies could be a result of different sampling strategies applied to a fractal estimator. For local measurements where small windows are used, the impacts of different sampling strategies on the resultant fractal dimensions could be high. This paper introduces a new sampling strategy, called the divisor-step method, which can be applied to the triangular prism method to compute the fractal dimension. The divisor-step method is designed to fully utilize the entire study area (window) for all steps for calculation, so that part of the study area will not be wasted in the calculation.

Using 4000 simulated surfaces and an IKONOS subset, the divisor-step method was compared with the two conventional approaches, the arithmetic-step and the geometric-step (varying coverage) methods. It was found that the geometric-step method (varying coverage) was less stable and less accurate than the other two methods for most theoretical dimensions and windows; hence, it is not recommended for use by the triangular prism method. The arithmetic-step method consistently yielded a higher dimension than the other two methods. It performed better when the surfaces were of lower complexity, but for surfaces of high complexity ($D = 2.7, 2.9$), the arithmetic-step method overestimated the fractal dimensions and sometimes yielded a value exceeding 3.0. On the other hand, the divisor-step method underestimated the fractal dimension values for surfaces of low complexity, but performed very well for surfaces of high complexity such as satellite images. The overall RMSE for the divisor-step method was also the lowest. Based on these results, it is recommended that the divisor-step method should be employed in fractal surface calculation algorithms, especially for complex urban remote sensing image characterization. The divisor-step method can be easily programmed and implemented in any fractal estimation algorithms.

Acknowledgments

References

Chust, G., Ducrot, D., Pretus, J.L., 2004. Land cover mapping with patch-derived landscape indices. Landscape and Urban Planning 69 (4), 439–449.

Clarke, K.C., 1986. Computation of the fractal dimension of topographic surfaces using the triangular prism surface area method. Computers & Geosciences 12 (5), 713–722.

De Cola, L., 1989. Fractal analysis of a classified Landsat scene. Photogrammetric Engineering & Remote Sensing 55 (5), 601–610.

De Jong, S.M., Burrough, P.A., 1995. A fractal approach to the classification of Mediterranean vegetation types in remotely sensed images. Photogrammetric Engineering & Remote Sensing 61 (8), 1041–1053.

Emerson, C.W., Lam, N.S.-N., Quattrochi, D.A., 2005. A comparison of local variance, fractal dimension, and Moran's I as aids to multi-spectral image classification. International Journal of Remote Sensing 26 (8), 1575–1588.

Goodchild, M.F., 1980. Fractals and the accuracy of geographical measures. Mathematical Geology 12, 85–98.

Jaggi, S., Quattrochi, D.A., Lam, N.S.-N., 1993. Implementation and operation of three fractal measurement algorithms for analysis of remote-sensing data. Computers & Geosciences 19 (6), 745–767.

Lam, N.S.-N., 2004. Fractals and scale in environmental assessment and monitoring. In: Sheppard, E., McMaster, R. (Eds.), Scale and Geographic Inquiry: Nature, Society, and Method. Blackwell Publishing, Oxford, UK, pp. 23–40.

Lam, N.S.-N., De Cola, L. (Eds.), 1993. Fractals in Geography. Prentice Hall, Englewood Cliffs, NJ, 308pp.

Lam, N.S.-N., Qiu, H.L., Quattrochi, D.A., Emerson, C.W., 2002. An evaluation of fractal methods for characterizing image complexity. Cartography and Geographic Information Science 29 (1), 25–35.

Lam, N.S.-N., Quattrochi, D.A., Qiu, H.L., Zhao, W., 1998. Environmental assessment and monitoring with image characterization and modeling system using multiscale remote sensing data. Applied Geographical Studies 2 (2), 77–93.

Liu, A.J., Cameron, G.N., 2001. Analysis of landscape patterns in coastal wetlands of Galveston Bay, Texas (USA). Landscape Ecology 16 (7), 581–595.

Mandelbrot, B.B., 1967. How long is the coast of Britain? Statistical self-similarity and fractional dimension. Science 156, 636–638.

Mandelbrot, B.B., 1975. On the geometry of homogeneous turbulence, with stress on the fractal dimension of isosurfaces of scalars. Journal of Fluid Mechanics 72 (2), 401–416.

Mandelbrot, B.B., 1983. The Fractal Geometry of Nature. W.H. Freeman, New York, NY, 480pp.

Myint, S.W., Lam, N.S.-N., Tyler, J.M., 2004. Wavelets for urban spatial feature discrimination: comparisons with fractal, spatial autocorrelation, and spatial co-occurrence approaches. Photogrammetric Engineering & Remote Sensing 70 (7), 803–812.

Myint, S.W., Lam, N.S.-N., 2005. Examining lacunarity approaches in comparison with fractal and spatial autocorrelation techniques for urban mapping. Photogrammetric Engineering & Remote Sensing 71 (8), 927–937.

Qiu, H.L., Lam, N.S.-N., Quattrochi, D.A., Gamon, J.A., 1999. Fractal characterization of hyperspectral imagery. Photogrammetric Engineering & Remote Sensing 65 (1), 63–71.

Quattrochi, D.A., Lam, N.S.-N., Qiu, H.L., Zhao, W., 1997. Image characterization and modeling system (ICAMS): a geographic information system for the characterization and modeling of multi-scale remote sensing data. In: Quattrochi, D.A., Goodchild, M.F. (Eds.), Scale in Remote Sensing and GIS. CRC Press, Boca Raton, FL, pp. 295–308.

Quattrochi, D.A., Emerson, C.W., Lam, N.S.-N., Qiu, H.L., 2001. Fractal characterization of multitemporal remote sensing data. In: Tate, N.J., Atkinson, P.M. (Eds.), Modelling Scale in Geographical Information Science. Wiley, New York, pp. 13–34.

Read, J.M., Lam, N.S.-N., 2002. Spatial methods for characterizing land cover and detecting land-cover changes for the tropics. International Journal of Remote Sensing 23 (12), 2457–2474.

Sun, W., 2006. Three new implementations of the triangular prism method for computing the fractal dimension of remote sensing images. Photogrammetric Engineering & Remote Sensing 72 (4), 373–382.

Sun, W., Xu, G., Gong, P., Liang, S., 2006. Fractal analysis of remotely sensed images: a review of methods and applications. International Journal of Remote Sensing 27 (22), 4963–4990.

Tate, N.J., 1998. Estimating the fractal dimension of synthetic topographic surfaces. Computers & Geosciences 24 (4), 325–334.

Turner, M.G., Ruscher, C.L., 1988. Changes in landscape patterns in Georgia, USA. Landscape Ecology 1 (4), 241–251.

Voss, R.F., 1988. Fractals in nature: from characterization to simulation. In: Barnsley, M.F., Devaney, R.L., Mandelbrot, B.B., Peitgen, H.-O., Saupe, D., Voss, R.F. (Eds.), The Science of Fractal Images. Springer, New York, pp. 21–70.

Zhao, W., 2001. Multiscale analysis for characterization of remotely sensed images. Ph.D. Dissertation, Louisiana State University, Baton Rouge, Louisiana, USA, 238pp.

Zhou, G., Lam, N.S.-N., 2005. A comparison of fractal dimension estimators based on multiple surface generation methods. Computers & Geosciences 31 (10), 1260–1269.